DOI: https://doi.org/10.37434/tpwj2023.07.02

FEATURES OF FORMATION AND TRANSFORMATION OF OXIDES IN FLASH-BUTT WELDING OF K76F RAILS

V.I. Shvets, I.V. Ziakhor, L.M. Kapitanchuk

E.O. Paton Electric Welding Institute of the NASU
11 Kazymyr Malevych Str., 03150, Kyiv, Ukraine

ABSTRACT

The transformation of oxide inclusions in flash-butt welding (FBW) of K76F rails was studied with the use of the Auger-microprobe JAMP 9500F of JEOL Company (Japan) with the X-ray energy dispersion spectrometer INCA Penta FET x3 mounted on it and involvement of the most informative methodologies of fractographic analysis. It is shown that high-temperature oxide inclusions without changing the aggregate state are removed as a flash. On the basis of silicon oxides on a molten surface in the welding process, easy fusible ferromanganese and in the near-contact layer — manganese silicates are formed. The heterogeneity of silicon distribution is the cause of formation of clusters of silicates and formation of "matt spots" in the near-contact layer.

KEYWORDS: flash-butt welding, KF76 rails, silicates, "matt spots"

INTRODUCTION

Nonmetallic inclusions (NI) violate the integrity of metal and, having excellent mechanical and physical properties, exert a significant impact on its mechanical and operational properties [1]. Modern converter rail steels are characterized by the presence of the following NI in the structure: globular sulphides and manganese oxides, in-line ferromanganese sulphides, complex oxides containing silicon, aluminium and calcium elongated along the direction of rolling. The listed NI represent non-removed products of deoxidation and desulfurization of steel [2].

In thermal deformation conditions of welding, it is possible to transform NI with a probable enhancement of their negative impact. In [3], the problem of flashing of ferromanganese sulphides in the near-contact layer of rails is considered. The flashing is caused by the existence of eutectics with a melting point of 1164 °C in the Fe–Mn–S system. It is shown that after flashing, the melt spreads along the structural boundaries. During cooling of welded joints, opening of metal may occur on the formed cast interlayers. Such a defect is manifested by the means of US testing. The joint in this case is recognized as defective. The danger is posed by cracking over these layers during operation after laying the rails in the track. Here it is recommended to use a welding mode, during which the heat input is reduced in order to hinder the process of flashing sulphides at the stage of coagulation before the spread of the melt along the intergranular boundaries [4].

Simple oxides, encountered in the metal of rails, are characterized as refractory — their melting point is much higher than the melting point of iron — 1538 °C. At the same time, the data of studying the state diagrams indicate the existence of easy fusible eutectics in oxide systems [5]. The presence of easy fusible eutectics gives grounds to suggest about a probable flashing of both complex oxides, as well as products of diffusion interaction of oxides with the matrix in FBW. The formation of a liquid phase with its subsequent crystallization may cause additional inner stresses in the metal and reduce the properties of joints.

The aim of the work was to establish the features of formation and transformation of oxide inclusions in rail steels in FBW.

PROCEDURE AND EQUIPMENT

The joints of K76F rails, produced in the K1000 machine for flash-butt welding by the technology developed at PWI of NASU, were considered [6]. The studies of NI were performed on the fracture surfaces of the joints after tests for static bending. The examinations of the microstructure of the fracture surface and determination of the chemical composition of structural components were conducted with the use of the Auger-microprobe JAMP 9500F of JEOL Company (Japan) with the X-ray energy dispersion spectrometer INCA Penta FET x3 of Oxford Instrument Company, mounted on it. The power of the primary electron beam was 10 KeV at a current of 0.5 nA for the SEM and EPMA methods and at a current of 10 nA for the Auger-electron spectroscopy method. The Auger-spectra were registered with the energy separation ability $\Delta E/E = 0.6$ %. Before the examinations, the surface of the specimens was subjected to

cleaning directly in the analysis chamber of the device by argon Ar+ ions etching with the energy of 1 keV during 10 min. The rate of SiO_2 etching over the reference witness specimen was 4 nm/min. The vacuum in the analysis chamber was within $5 \cdot 10^{-6}$–$5 \cdot 10^{-7}$ Pa. Metallographic examinations were performed in the optical NEOPHOT 32 microscope, equipped with a digital camera. Microstructure was revealed by etching of preliminary polished specimens in a 4 % alcohol HNO_3 solution.

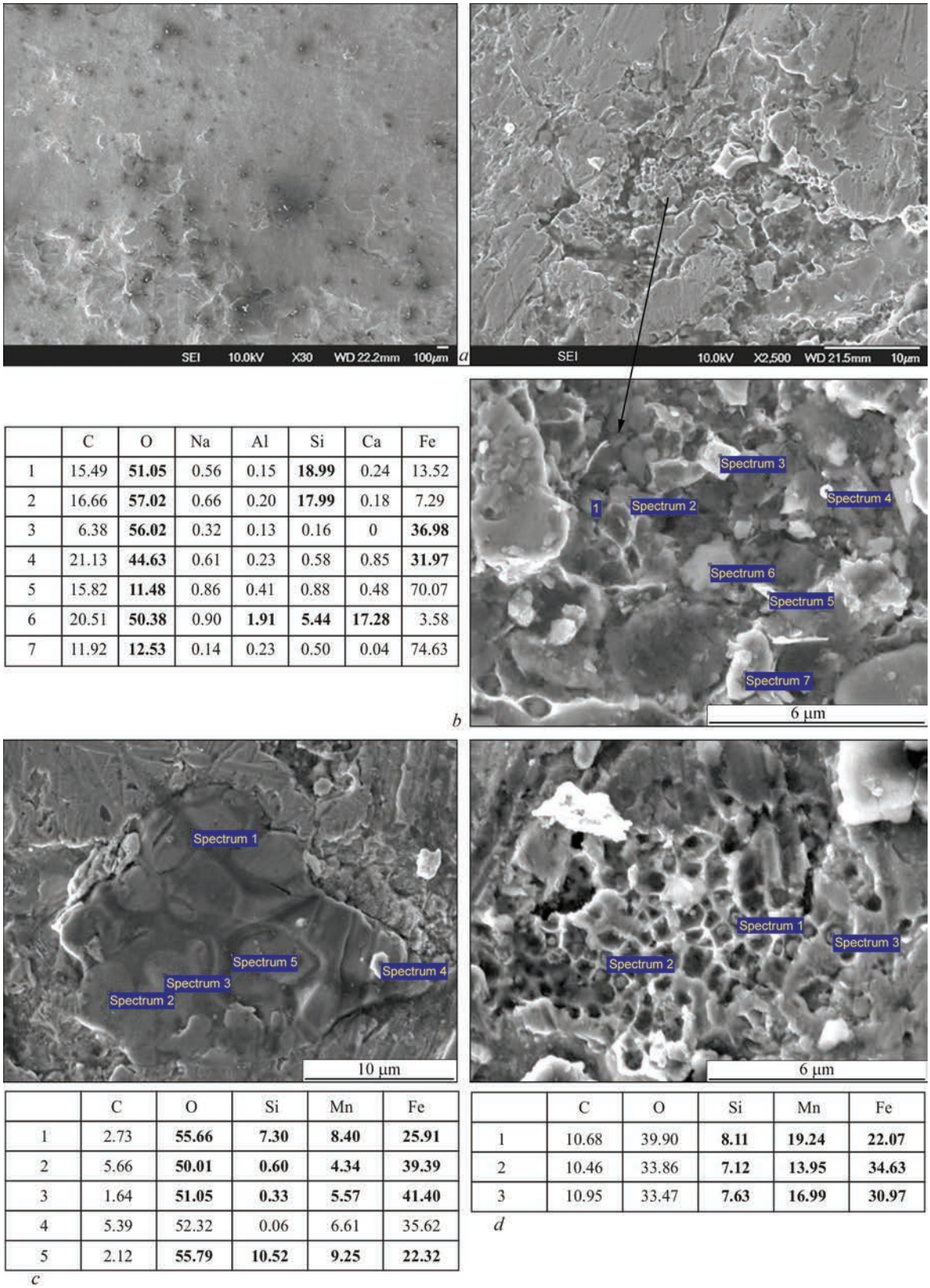

	C	O	Na	Al	Si	Ca	Fe
1	15.49	**51.05**	0.56	0.15	**18.99**	0.24	13.52
2	16.66	**57.02**	0.66	0.20	**17.99**	0.18	7.29
3	6.38	**56.02**	0.32	0.13	0.16	0	**36.98**
4	21.13	**44.63**	0.61	0.23	0.58	0.85	**31.97**
5	15.82	**11.48**	0.86	0.41	0.88	0.48	70.07
6	20.51	**50.38**	0.90	**1.91**	**5.44**	**17.28**	3.58
7	11.92	**12.53**	0.14	0.23	0.50	0.04	74.63

b

	C	O	Si	Mn	Fe
1	2.73	**55.66**	**7.30**	**8.40**	**25.91**
2	5.66	**50.01**	**0.60**	**4.34**	**39.39**
3	1.64	**51.05**	**0.33**	**5.57**	**41.40**
4	5.39	52.32	0.06	6.61	35.62
5	2.12	**55.79**	**10.52**	**9.25**	**22.32**

c

	C	O	Si	Mn	Fe
1	10.68	39.90	**8.11**	**19.24**	**22.07**
2	10.46	33.86	**7.12**	**13.95**	**34.63**
3	10.95	33.47	**7.63**	**16.99**	**30.97**

d

Figure 1. Microstructure of fracture surface in the area of "cold welding": *a* — general appearance; *b–d* — results of X-ray microanalysis of nonmetallic inclusions (at.%)

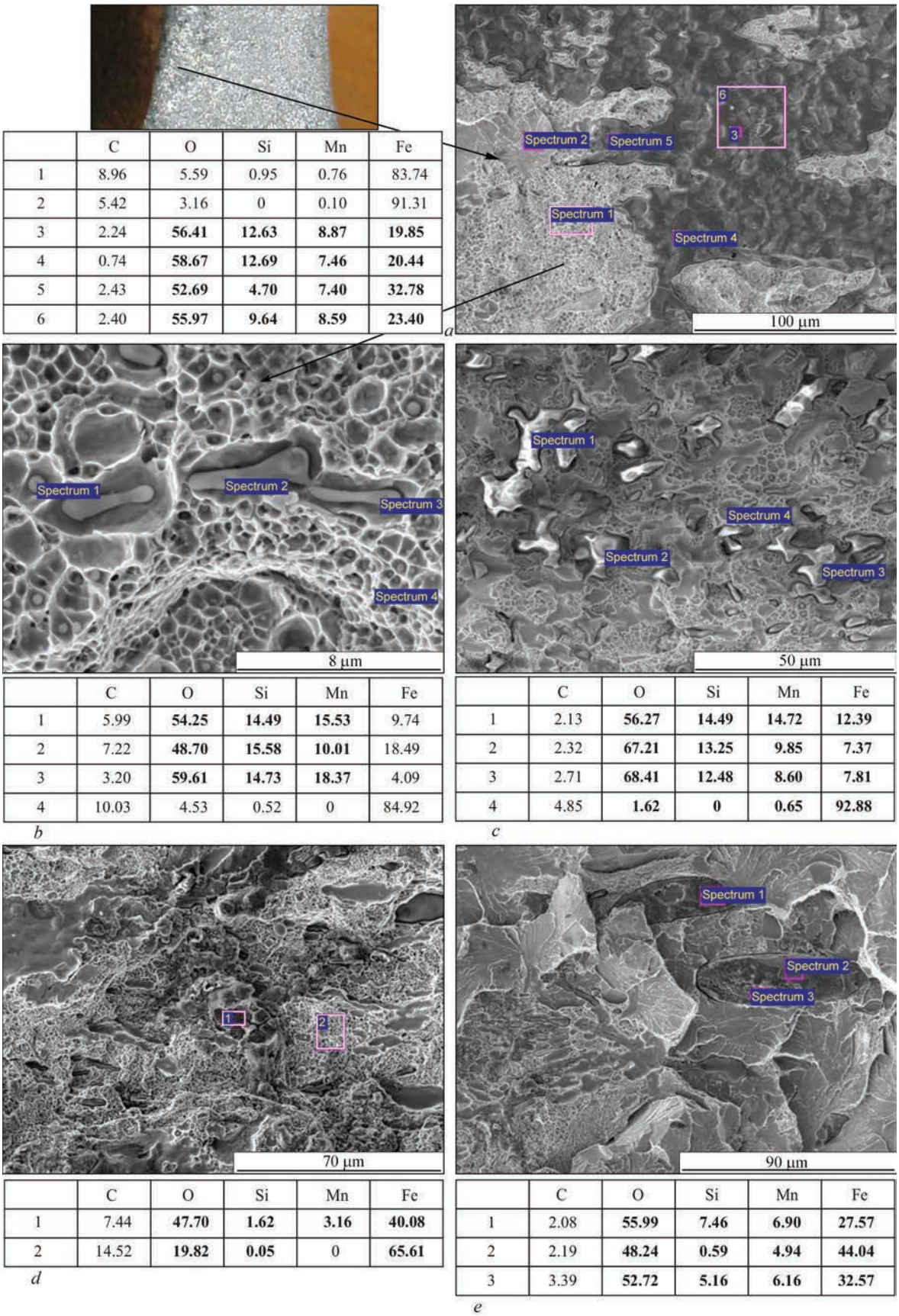

	C	O	Si	Mn	Fe
1	8.96	5.59	0.95	0.76	83.74
2	5.42	3.16	0	0.10	91.31
3	2.24	**56.41**	**12.63**	**8.87**	**19.85**
4	0.74	**58.67**	**12.69**	**7.46**	**20.44**
5	2.43	**52.69**	**4.70**	**7.40**	**32.78**
6	2.40	**55.97**	**9.64**	**8.59**	**23.40**

a

	C	O	Si	Mn	Fe
1	5.99	**54.25**	**14.49**	**15.53**	9.74
2	7.22	**48.70**	**15.58**	**10.01**	18.49
3	3.20	**59.61**	**14.73**	**18.37**	4.09
4	10.03	4.53	0.52	0	84.92

b

	C	O	Si	Mn	Fe
1	2.13	**56.27**	**14.49**	**14.72**	**12.39**
2	2.32	**67.21**	**13.25**	**9.85**	**7.37**
3	2.71	**68.41**	**12.48**	**8.60**	**7.81**
4	4.85	**1.62**	**0**	**0.65**	**92.88**

c

	C	O	Si	Mn	Fe
1	7.44	**47.70**	**1.62**	**3.16**	**40.08**
2	14.52	**19.82**	**0.05**	0	**65.61**

d

	C	O	Si	Mn	Fe
1	2.08	**55.99**	**7.46**	**6.90**	**27.57**
2	2.19	**48.24**	**0.59**	**4.94**	**44.04**
3	3.39	**52.72**	**5.16**	**6.16**	**32.57**

e

Figure 2. Microstructure of fracture surface in the "lack of fusion" area: *a* — general appearance; *b*–*e* — results of X-ray microanalysis of nonmetallic inclusions (at.%)

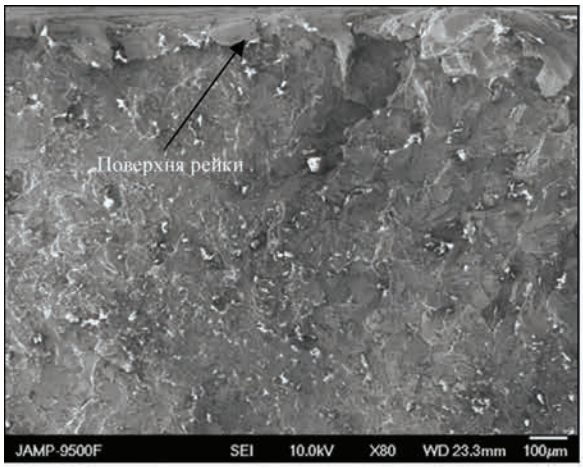

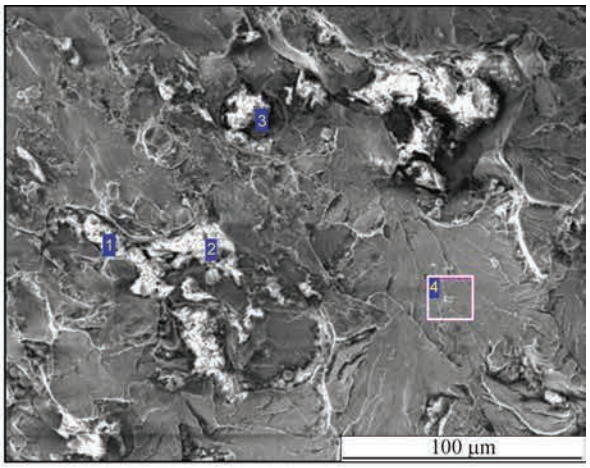

	C	O	Na	Mg	Al	Si	S	Cl	K	Ca	Fe
1	65.54	**23.93**	0.62	0.26	**1.32**	**1.04**	0.50	0.26	0.32	**2.54**	**3.70**
2	32.24	**33.83**	0.31	0.51	**2.08**	**1.09**	0.40	0.50	0.23	**1.29**	**27.52**
3	65.48	5.79			**4.76**	**16.05**	1.04		2.05	**1.80**	**3.04**
4	8.34	6.74			0.40	0.92					83.60

a

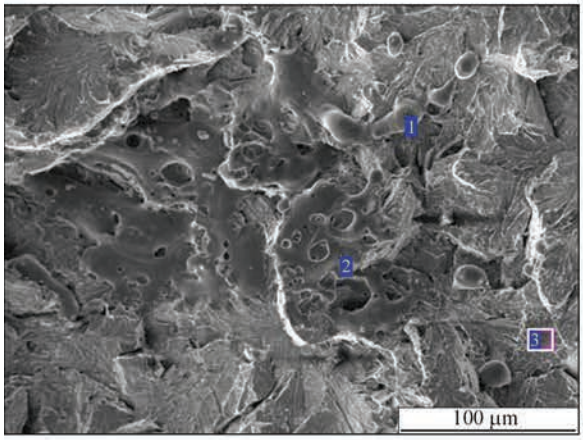

b

	C	O	Si	Mn	Fe
1	7.57	**23.32**	0.21	0	**68.89**
2	3.09	**57.02**	0.98	0.10	**38.82**
3	5.43	3.53	1.37	0.23	89.43

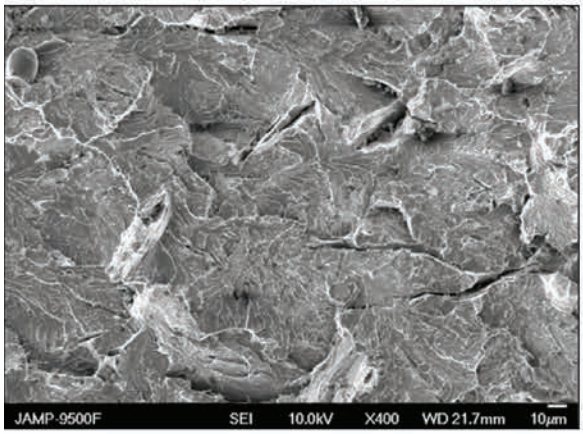

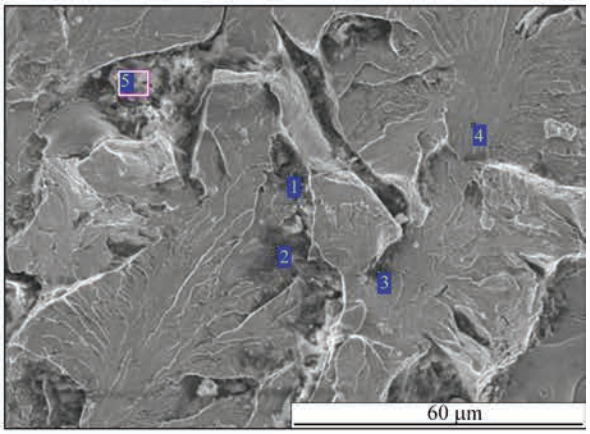

	C	O	Na	Al	Si	S	Ca	Fe	Cu
1	**71.29**	13.13	0.23	0.29	0.92	–	0.61	13.53	–
2	**73.69**	14.97	–	**1.34**	0.68	–	–	9.32	–
3	**70.75**	17.11	0.10	**1.17**	0.81	0.23	0.69	9.16	–
4	7.85	3.36	–	–	**1.26**	–	–	**87.53**	–
5	**67.52**	**24.46**	–	**2.13**	**1.29**	0.15	1.08	2.96	0.27

c

Figure 3. Microstructure of fracture surface and results of X-ray microanalysis of nonmetallic inclusions in the area of incomplete removal of the melt as a flash: *a* — refractory oxides; *b* — iron oxides; *c* — secondary cracks (at.%)

RESEARCH RESULTS AND DISCUSSION

The fracture surface of the rail joints produced on the optimal mode is crystalline. On the opened welding defects formed in the case of deviation of the mode parameters from the optimal ones, the surface is visually flat. To get a more complete notion of the formation and transformation of NI along with the study on the surface of the crystalline fracture and in the near-contact layer of the joint, the formation of structural components in the regions of such welding defects as "cold welding" and "lack of fusion" was considered [7].

The peculiarity of "cold welding" consists in the insufficient heating of rail before upsetting and, as a consequence, a partial flashing of the end. The fracture surface in this region of opening is flat (Figure 1). Within the flat surface, refractory nonmetallic inclusions, such as oxides of silicon, aluminium, complex oxides, including aluminium, calcium, silicon, globular iron oxides are observed (Figure 1, *b*). Near the oxides, flashed-type silicates in the form of films (Figure 1, *c*) and clusters of tiny globular particles are encountered, the size of which amounts to fractions of a micron (Figure 1, *d*). Globular particles are a product of ferromanganese film fragmentation and cause a locally tough nature of the fracture.

Lacks of fusion are formed in the places of more intense penetration. On the fracture surface, lacks of fusion are distinguished as smooth regions, that do not have a distinct crystalline structure. According to the results of X-ray microanalysis, a layer of ferromanganese silicate (Figure 2, *a*, spectrum 3) makes a bulk part of the lack of fusion surface. Within the lack of fusion, films of an easy fusible iron oxide — wüstite are encountered (Figure 2, *d*, spectrum 1). In the layers of ferromanganese silicates, as well as in the wüstite films, the clusters of globular particles with the size of less than 1 μm are revealed (Figure 2, *b*, spectrum 1). The particles are films fragmentation products of ferromanganese silicates and wüstite, respectively. A negligible size of particles causes a tough nature of the fracture in the regions of their location.

In the transition zone on the boundary of the lack of fusion area with a crystalline fracture, the inclusions of flashed-type ferromanganese silicates with a reduced content of iron compared to the layer of ferromanganese silicates are encountered (Figure 2, *c*). There, films of ferromanganese silicates with elevated ferro content are encountered (Figure 2, *e*).

As is seen, the structural components observed on the surface of the lack of fusion, belong to the Si–Mn–Fe–O system. The prerequisite for their formation is obviously the presence of eutectics with a temperature of 1178 and 1117 °C [4] in the SiO_2–FeO system, as well as unlimited solubility in the MnO–FeO system [8]. Obviously, that in the process of welding, an oxidation of metal of flashed rail ends occurs. On the surface, first of all, an easy fusible iron oxide (wüstite) with some content of manganese is formed. The interaction of the near-surface silicon oxide with iron oxide and an increase in the content of diffusion-active manganese leads to the formation of ferromanganese silicates. The source of manganese can be both the rail metal, as well as its refractory oxides. The presence and distribution of silicon oxide inclusions in the surface layer determines the chemical composition and morphology of structural components of the lack of fusion surface.

In FBW, the rail metal, flashed on the ends, is removed during upsetting beyond the boundaries of a workpiece cross-section. Together with the melt, oxidation products of the surface layer and NI, contained in the melt, are removed. While studying the fracture area with an incomplete removal of the melt, numerous inclusions of complex oxides of aluminium, calcium and silicon were found (Figure 3, *a*). There, globular and film oxides of iron are encountered (Figure 3, *b*). A typical feature of the microstructure is secondary cracks of up to 100 μm in size (Figure 3, *c*). The cracks contain small oxide inclusions observed on the background of carbon content, elevated up to 50–70 at.%. A high carbon content is associated with its redistribution in thermal-deformation conditions of welding and filling the volumes on the boundary of nonmetallic inclusions and matrix [9].

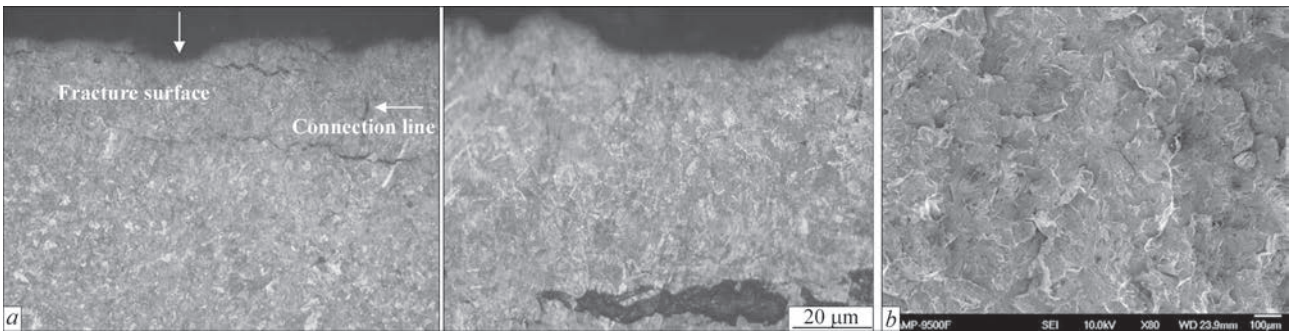

Figure 4. Microstructure of near-surface layer (*a*) and fracture surface (*b*)

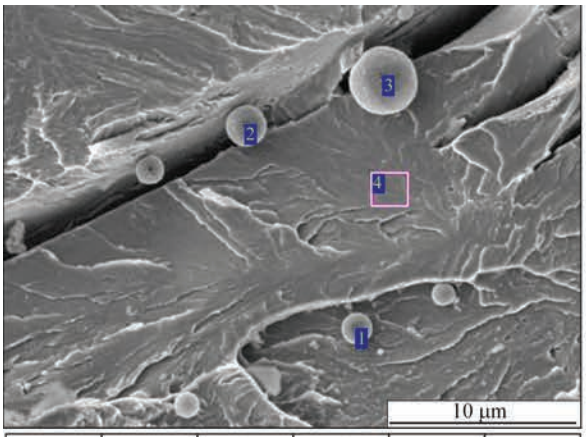

	C	O	Si	Mn	Fe
1	0.62	**28.07**	0.18	0.47	**70.66**
2	0.80	**27.63**	0	0.62	**70.95**
3	0.57	**28.07**	0.52	1.30	**69.55**
4	0.76	0.93	0.36	0.96	96.99

a

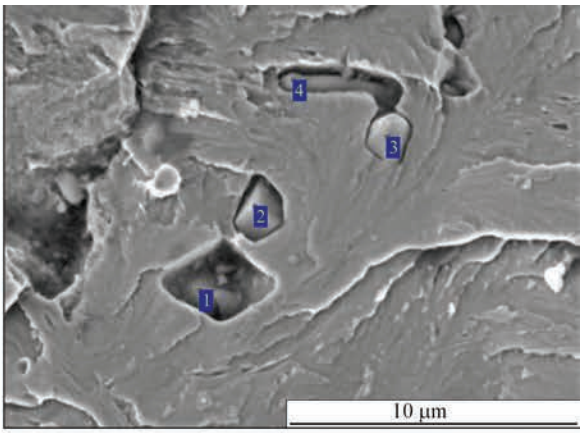

	C	O	Al	Si	S	Mn	Fe	Cu
1	11.05	8.09	0.32	1.56			78.97	
2	23.67	4.65		0.17	**31.11**	**32.75**	3.84	3.81
3	10.29			0	**41.72**	**39.44**	3.83	4.73
4	18.91	5.62		0.18	**30.70**	**32.47**	6.01	6.11

b

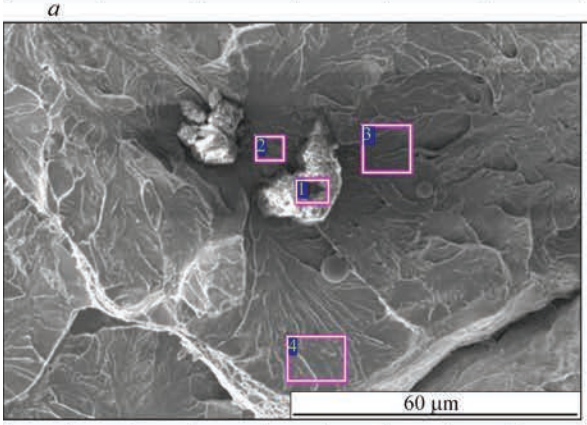

	C	O	Al	Si	S	Ti	Mn	Fe
1	**50.50**	**35.71**	0.61	0.47	0.54	**10.41**	0	1.66
2	18.63	8.41	0.20	0.52	0.18	0.59	0.60	69.77
3	9.37	1.49	0.13	0.63	0	0	0.67	87.39
4	8.22	2.62	0.11	0.74	0.06	0.13	0	87.88

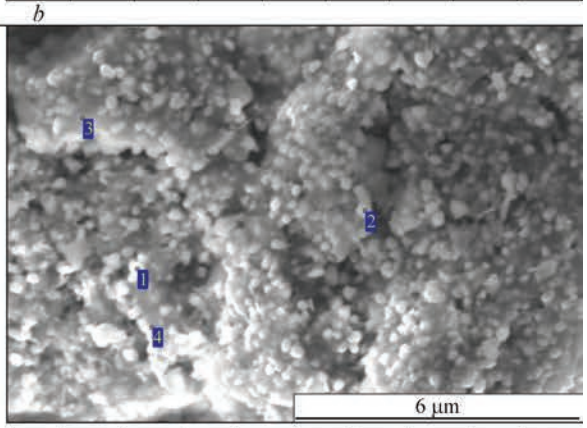

	C	O	Al	Si	S	Ca	Ti	Mn	Fe
1	**30.17**	**52.28**	0.29	0.45	0.15	0.29	**13.54**	0.14	2.54
2	**23.99**	**57.50**	0.78	0.33	0.13	0	**15.91**	0.12	1.23
3	**56.19**	**34.40**	0.33	0.42	0.88	0.14	**5.79**	0.05	1.54
4	**61.43**	**29.82**	0.45	0.72	0.33	0.01	**5.96**	0.07	1.09

c

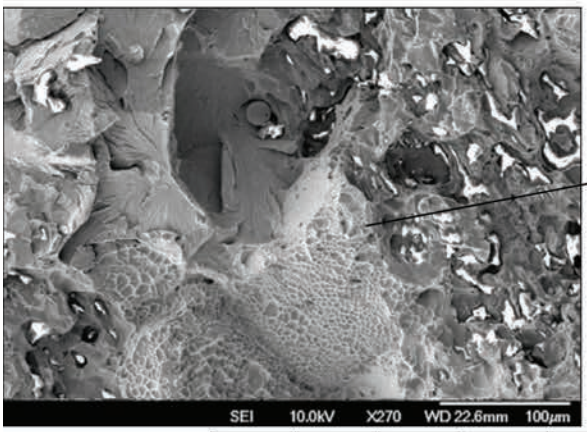

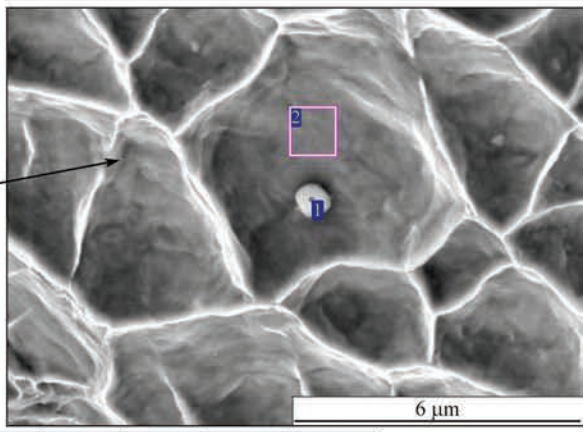

	C	O	Al	Si	S	Ti	Mn	Fe
1	19.24	**5.66**	0.42	0.24	**30.12**	0.67	**33.81**	**9.84**
2	5.67	1.28	0	0.59	0	0	1.04	**91.42**

d

Figure 5. Results of X-ray microanalysis of nonmetallic inclusions on the surface of crystalline fracture (at.%): *a* — iron oxides; *b* — manganese oxides; *c* — titanium carbon oxides; *d* — ferromanganese sulphides

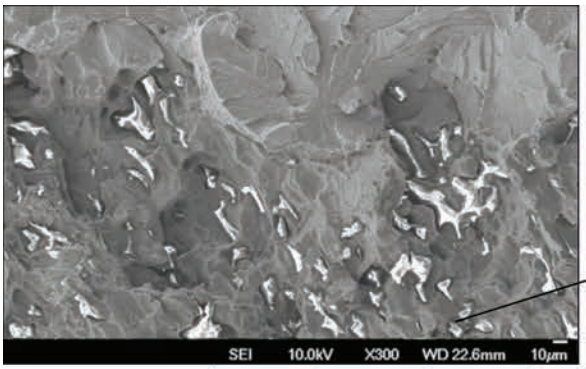

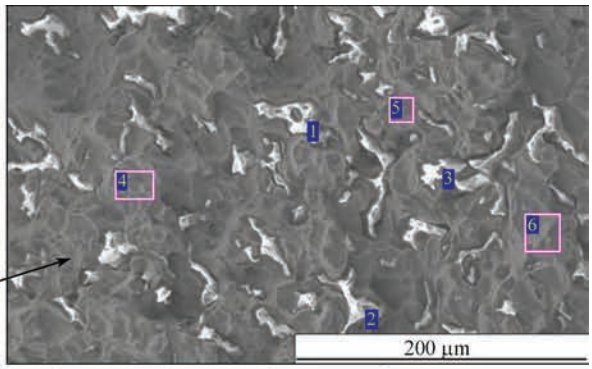

	C	O	Al	Si	Mn	Fe
1	3.27	**66.66**	**1.11**	**16.48**	**11.61**	0.86
2	3.36	**61.08**	**3.15**	**16.70**	**14.73**	0.99
3	2.41	**68.91**	**1.32**	**16.39**	**6.90**	0.90
4	4.43	1.57	0.11	0	0.80	93.09
5	5.51	0.86	0	0.18	0.81	90.76
6	4.70	1.50	0	0.15	1.11	92.54

a

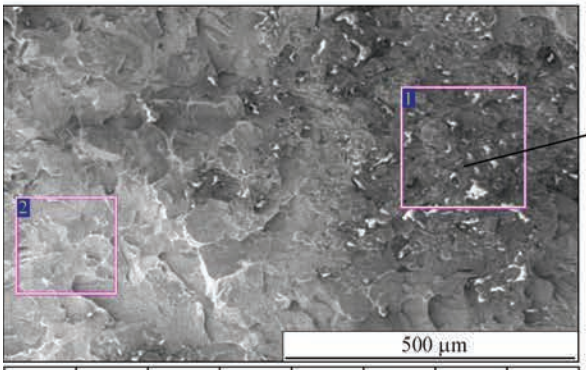

	C	O	Al	Si	Cr	Mn	Fe
1	14.43	21.93	0.11	5.76	0.34	5.47	51.96
2	7.01	1.63	0.05	0.41	0.34	1.45	89.11

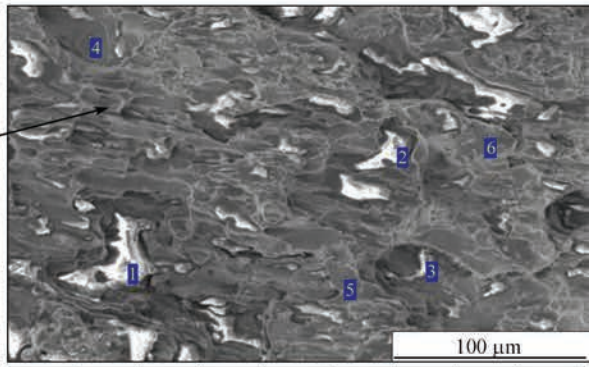

	C	O	Na	Al	Si	Cr	Mn	Fe
1	2.88	**66.74**	0	0	**18.05**	0	**10.32**	2.01
2	31.24	**50.68**	0.47	0.16	**10.67**	0.04	**5.85**	0.89
3	3.16	**59.39**	0.25	0.06	**18.88**	0.04	**15.63**	2.60
4	7.85	1.74	0	0	0.73	0	0.71	**88.97**
5	8.81	4.65	0	0.16	0.81	0.05	1.50	**84.02**
6	3.88	1.74	0.29	0	0.51	0	0.08	**93.51**

b

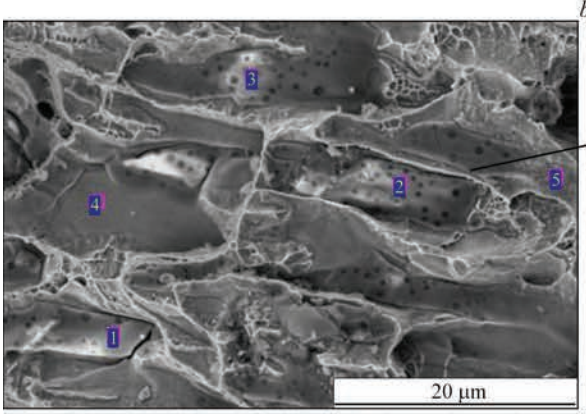

	C	O	Al	Si	S	Cr	Mn	Fe
1	1.72	**59.34**	0.16	**17.06**	0.33	0.27	**18.95**	2.17
2	1.85	**61.66**	0.21	**16.54**	0.20	0.05	**17.76**	1.75
3	1.96	**63.29**	0.04	**16.14**	0.05	0	**17.06**	1.46
4	1.28	0.98	0.05	0.20	0	0	1.23	96.27
5	11.57	17.56	0.31	3.96	0.36	0	5.84	60.40

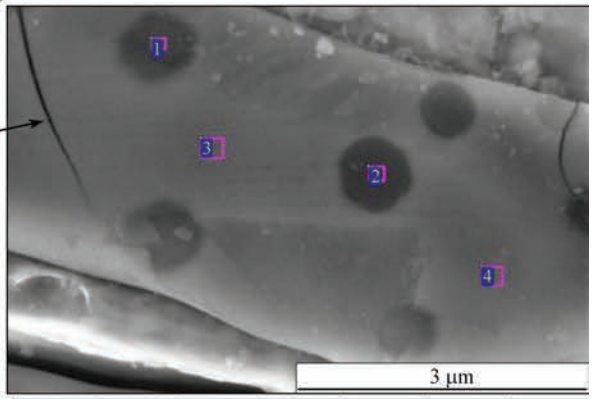

	C	O	Al	Si	Mn	Fe
1	1.99	51.28	0	**20.57**	1.81	24.35
2	2.10	62.25	0.06	**23.36**	3.49	8.74
3	0.68	58.26	0.22	**16.10**	21.05	3.69
4	1.91	59.21	0.11	**16.63**	18.96	3.17

c

Figure 6. Results of X-ray microanalysis of silicates of the near-contact layer of the rail joint (at.%): *a* — manganese aluminosilicates; *b*, *c* — manganese silicates

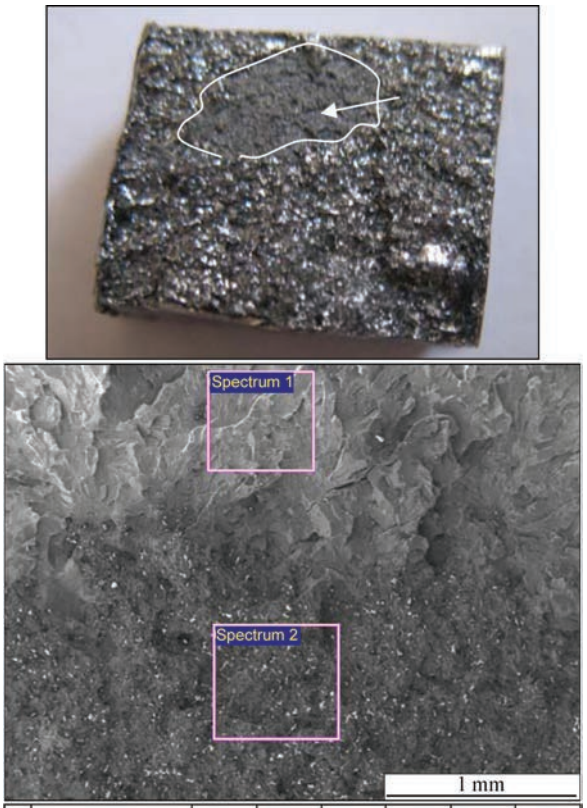

	Notes	C	O	Al	Si	Mn	Fe
1	Facets of spalling	8.34	2.74	0	0.25	0.13	88.55
2	Spot	7.01	16.52	0.45	4.08	5.86	66.08

Figure 7. "Matt spots" on the fracture surface of rail joints and results of X-ray microanalysis of surfaces from the area (at.%)

On the crystalline surface of the fracture, the microstructure represents facets of intragranular spalling with elements of plastic deformation: tongues, tear ridges (Figure 4, *b*). In the microstructure, tiny inclusions of manganese sulphide (Figure 5, *b*), globular inclusions of iron oxide (Figure 5, *a*), inclusions of oxides of alloying elements, in particular, titanium carbon oxides (Figure 5, *c*) are present. There, clusters of tiny sulphides (Figure 5, *c*) — fragmentation products of an easy fusible film (Fe, Mn)S are encountered, that is formed in the near-contact layer [3].

Along with the high-temperature oxides, on the fracture surface, flashed-type manganese silicates and alumosilicates of up to 30 μm in size (Figure 6, *a*, *b*) are observed. It is shown, that they have a cast structure (Figure 6, *c*). Unlike a layer of ferromanganese silicates on the lack of fusion surface, the content of iron in them is insignificant. The main crack during fracture passes at a distance of about 20–50 μm from the joint line (Figure 4, *a*). The transformation of nonmetallic inclusions, present on the surface of the crystalline fracture, apparently occurs in the layer of non-flashed metal. Considering that in the SiO_2–MnO system there are eutectics with a temperature of 1250 and 1315 °C [4], the formation of manganese silicates in the near-contact layer, apparently, occurs due to the diffusion interaction of surface-active manganese in iron with silica-containing oxides.

The inclusions of silicates often form clusters. Considering that opening of the rail metal during loading occurs along the weakened boundary of silicates with the matrix, as is seen in the fracture microstructure (Figure 6, *a*, *b*), the places of clusters of silicates in the normative documents are attributed to defects of welded joints that are classified as "matt spots" (Figure 7). Their appearance in the fracture microstructure is predetermined by the peculiar distribution of silicon oxide in the rail metal. Some amount of "matt spots" in the rail joints is acceptable. However, the total area should not be more than 15 mm^2 [10].

CONCLUSIONS

1. In welding of rails, high-temperature oxide inclusions, in addition to silicon oxide, transfer into a flashed layer and they are removed as a flash during upsetting without changing the aggregate state.

2. The existence of easy fusible eutectics with a temperature of 1178, 1117, 1250 and 1315 °C in the oxide SiO_2–FeO and MnO–FeO systems, respectively, as well as unlimited solubility in the MnO–FeO system is a prerequisite for the formation of manganese silicates on the surface of flashed rail ends during welding and in the near-contact layer of the joint.

3. Ferromanganese silicates on the flashed ends of the rails are formed as a result of the interaction of easy fusible iron oxide with the inclusions of silicon oxide and the subsequent diffusion of manganese from the rail metal. The welding technology involves the removal of ferromanganese silicates together with the melt as a flash during upsetting.

4. Manganese silicates in the near-contact layer of the joint are a product of diffusion interaction of surface-active manganese in iron with silica-containing oxide inclusions. Inclusions of manganese silicates often form clusters as a result of a nonuniform distribution of silicon oxides in the rail metal. Due to a weak adhesion to iron, the clusters of silicates affect the results of testing joints on impact toughness and static bending and are classified as defects of welded joints, the so-called "matt spots". Their total area is limited and should not exceed 15 mm^2 [10].

REFERENCES

1. Gubenko, S.I., Oshkaderov, S.P. (2016) *Nonmetallic inclusions in steel.* Kyiv, Naukova Dumka [in Russian].
2. Levchenko, N.V. (2006) Change of nonmetallic inclusions in manufacture of rails. *Metallurgicheskaya i Gornorudnaya Promyshlennost,* **2**, 63–65 [in Russian].
3. Kuchuk-Yatsenko, S.I., Didkovsky, A.V., Shvets, V.I. et al. (2016) Flash-butt welding of high-strength rails of nowadays

production. *The Paton Welding J.,* (**5–6**), 4–12. DOI: https://doi.org/10.15407/tpwj2016.06.01
4. Kuchuk-Yatsenko, S.I., Didkovsky, O.V., Bogorsky, M.V. et al. (2002) *Method of frash-butt welding.* Pat. 46820 Ukraine, Int. Cl. 6 B23K11/04, C2, Publ. 17.06.2002
5. Galakhov, F.Ya. (1991) *State diagrams of refractory oxide systems:* Refer. Book. Leningrad. Nauka [in Russian].
6. Kuchuk-Yatsenko, S., Shvets, V., Didkovsky, A. et al. (2016) Flash-butt welding of high-strength rails. Mining Informatics. *Automation and Electrical Engineering*, 528(**4**), 40–48.
7. Kuchuk-Yatsenko, S.I., Lebedev, V.K. (1976) *Flash-butt welding.* Kyiv, Naukova Dumka [in Russian].
8. Javojskij, V.I. (1969) *Theorie der Stahlerzeugung*. VEB Deutscerher Verlag fur Grundstoffindustrie. Leipzig.
9. Aksenova, K.V., Gromov, V.E., Ivanov, Yu.F. et al. (2017) Carbon redistribution under deformation of steels with bainite and martensite structures. *Izvestiya. Ferrous Metallurgy*, 60(**7**), 544–548 [in Russian]. DOI: https://doi.org/10.17073/0368-0797-2017-7-544-548.
10. TUU 24.1-40075815-002:2016: *New welded rails for railways* [in Ukrainian].

ORCID
V.I. Shvets: 0000-0003-4653-7453,
I.V. Ziakhor: 0000-0001-7780-0688,
L.M. Kapitanchuk: 0000-0002-8624-2590

CONFLICT OF INTEREST
The Authors declare no conflict of interest

CORRESPONDING AUTHOR
I.V. Ziakhor
E.O. Paton Electric Welding Institute of the NASU
11 Kazymyr Malevych Str., 03150, Kyiv, Ukraine.
E-mail: zyakhor2@ukr.net

SUGGESTED CITATION
V.I. Shvets, I.V. Ziakhor, L.M. Kapitanchuk (2023) Features of formation and transformation of oxides in flash-butt welding of K76F rails. *The Paton Welding J.*, **7**, 16–24.

JOURNAL HOME PAGE
https://patonpublishinghouse.com/eng/journals/tpwj

Received: 22.05.2023
Accepted: 06.09.2023